# Early-time kinetics of ordering in the presence of interactions with a concentration field

H. P. Fischer and W. Dieterich
*Fakultät für Physik, Universität Konstanz, D-78434 Konstanz, Germany*
(Received 26 March 1997)

The interplay between ordering and spinodal decomposition in binary systems is investigated within time-dependent Ginzburg-Landau theory for two coupled order parameters describing structural order and the concentration. The linearized theory suggests a classification of possible instabilities, and the associated mode spectra display marked deviations from the predictions of the conventional Cahn-Hilliard theory. Numerical calculations for a simplified model indicate the possibility of sequences of instabilities. We also show that the relative magnitude of kinetic coefficients can have a profound influence on the observed domain patterns. [S1063-651X(97)11411-8]

PACS number(s): 64.60.−i

## I. INTRODUCTION

Consider a binary system that undergoes a first-order phase transition where the disordered mixture transforms to an ordered structure via diffusional motions of atoms or molecules. Physical examples include many solid materials such as metallic alloys [1] or adsorbed layers on solid substrates [2], but are also known in the field of complex fluids [3].

In the following we assume the transition to be strongly of first order (as, for example, in the Li-Al or Mg-In alloy system), i.e., to display a pronounced miscibility gap in the $(T,c)$ plane of the phase diagram. Here $T$ denotes temperature and $c$ is an atomic concentration variable. A common way to study the dynamics of the transition is to quench the system from an initial disordered equilibrium phase, the $\alpha$ phase, at temperature $T_i$ to a final temperature $T_f$ inside the two-phase region separating the $\alpha$ phase from the ordered $\beta$ phase. The subsequent time evolution of the system will then be governed by an interplay of ordering and phase separation. In particular, after a quench into the regime where the $\alpha$ phase is unstable, spontaneous growth of fluctuations of the underlying structural order parameter $\psi$ and growth of long-wavelength concentration fluctuations become competing processes. Previous work, based on thermodynamic arguments [4] and on studies of microscopic kinetic models [5–7], has shown that this can lead to a sequence of instabilities and to a variety of transient structures in the early stages of the process. In fact, processes of homogeneous (''congruent'' [5]) ordering and subsequent decomposition have been detected experimentally, for example, in the $\alpha$-$\delta'$ transition of Li-Al alloys, although the question concerning the nature of the second process seems to be open up to now [8,9].

In this paper we investigate a time-dependent Ginzburg-Landau model that provides a minimal description of the interplay of ordering and spinodal decomposition. In the language of Hohenberg and Halperin [10] we will be concerned with ''model C,'' which in its simplest form consists of coupled equations of motion for a one-component, nonconserved order parameter field $\psi(\mathbf{r},t)$ and a conserved concentration field $c(\mathbf{r},t)$. In the absence of thermal noise, these equations take the form

$$\frac{\partial c}{\partial t} = \Gamma_c \Delta \frac{\delta F}{\delta c}, \tag{1}$$

$$\frac{\partial \psi}{\partial t} = -\Gamma_\psi \frac{\delta F}{\delta \psi}, \tag{2}$$

where $F[c,\psi]$ denotes the underlying Ginzburg-Landau free-energy functional and $\Gamma_\psi$ and $\Gamma_c$ are phenomenological kinetic coefficients. The late-stage dynamics of model C have been investigated recently by a number of authors [11–13]. By contrast, we will focus here on the early stages before domain coarsening becomes the dominant process, where our model shows more structure than the conventional Cahn-Hilliard theory (''model B''). After discussing the main properties of the free energy surface and the reduction of our equations of motion to a dimensionless form (Sec. II), we present in Sec. III the linearized theory, from which we infer a systematic classification of different kinetic instabilities. Their physical significance is confirmed in subsequent numerical solutions of the nonlinear problem (Sec. IV). Thereby, we show that after a sudden quench from the $\alpha$ phase a temporal sequence of instabilities can occur. In fact, for the case of fast structural relaxation we observe ''congruent ordering'' [5] prior to an unstable growth of concentration fluctuations, which, however, remain strongly coupled to the structural order parameter. Both of these successive instabilities have a character as predicted by the linearized theory. By contrast, in the case of slow structural relaxation, ordering and phase separation occur simultaneously. As a result, we obtain strongly fluctuating patterns whose structure factors cannot be described by the linearized theory in any relevant time interval. The distinction of fast and slow structural relaxation becomes even more relevant if the state right after the quench is close to the ''conditional'' spinodal [4]. In this way we find different kinetic scenarios depending on the quench conditions and on the relative magnitude of the kinetic coefficients $\Gamma_c$ and $\Gamma_\psi$. A summary of our results together with a discussion of their experimental relevance is given in the last section.

 

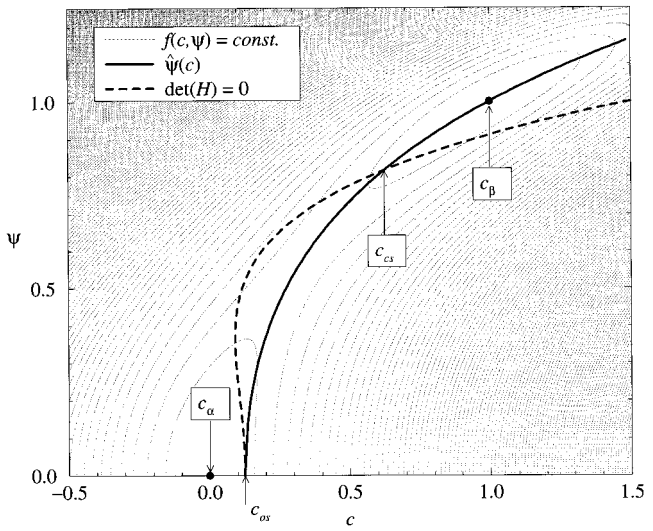


FIG. 1. Contourplot for the thermodynamic potential Eq. (6) in the $(c,\psi)$ plane ($\psi \geqslant 0$). Here the compositional variable $c$ is chosen such that the disordered phase has $c_\alpha = 0$, whereas the ordered phase corresponds to $c_\beta = \psi_\beta = 1$. The curve $\hat{\psi}(c)$, which satisfies $f_\psi = 0$, is represented by the solid line. The ordering spinodal is reached at $c_{os} = 0.125$. The dashed curve corresponds to $\det \mathbf{H} = 0$, where $\mathbf{H}$ is defined by Eq. (15); it is the limit of the unstable region of the free-energy surface. The intersection of the dashed and the solid line defines the conditional spinodal at $c_{cs} = 0.625$.

## II. GINZBURG-LANDAU MODEL

Our starting point is a free-energy functional $F[c,\psi]$ of the Ginzburg-Landau form

$$F[c,\psi] = \int d^3r \left[ f(c,\psi) + \frac{1}{2} K_c (\nabla c)^2 + \frac{1}{2} K_\psi (\nabla \psi)^2 \right], \tag{3}$$

where, for simplicity, we assume that the free-energy density $f$ of a uniform state satisfies $f(c,\psi) = f(c,-\psi)$. This symmetry condition applies, for example, to metallic alloys, where the ordered state can be described by the preferential occupation of one of two equivalent sublattices.

At this point let us further specify the general character of the function $f(c,\psi)$. First, considering a fixed temperature $T = T_f$, it should allow for coexistence of a stable disordered phase ($\psi_\alpha = 0$) with concentration $c_\alpha$ and an ordered phase $(c_\beta, \psi_\beta)$. Hence the grand canonical potential $f - \mu c$, where $\mu$ denotes the chemical potential, displays local minima at the corresponding points in the $(c,\psi)$ plane (see Fig. 1), with $f_\alpha - \mu c_\alpha = f_\beta - \mu c_\beta$. To be specific, suppose that ordering is favored upon increasing the concentration, and therefore $c_\beta > c_\alpha$. Next, we assume a point $c_{os} > c_\alpha$ on the $c$ axis in Fig. 1, which corresponds to the ordering spinodal, such that $(f_{\psi\psi})_{\psi=0} \gtrless 0$ for $c \lesseqgtr c_{os}$, respectively. Here we use the notation $(\partial/\partial\psi) f \equiv f_\psi$, etc. Finally, for fixed $c$, $f$ has a minimum with respect to $\psi$ along a curve $\hat{\psi}(c)$ in the $(c,\psi)$ plane, which satisfies $f_\psi = 0$ and necessarily passes the ordered state $(c_\beta, \psi_\beta)$. This curve is indicated in Fig. 1 by the solid line. It is natural to assume that this curve also meets the ordering spinodal $(c_{os}, \psi = 0)$. [In fact, by expanding $f(c,\psi)$ it is seen that a curve satisfying $f_\psi = 0$ enters the point $(c_{os}, \psi = 0)$ with vertical slope.] Clearly, at that point, the concentration-dependent free-energy density of the disordered phase, $f_\alpha(c) = f(c, \psi = 0)$, and the ''conditional free-energy density'' [4] of the ordered phase, $f_\beta(c) = f(c, \hat{\psi}(c))$, are equal. A simple form for $f(c,\psi)$ consistent with these requirements is

$$f(c,\psi) = f_0(c) + f_1(\psi) - \eta c \psi^2, \tag{4}$$

where

$$f_1(\psi) = r\psi^2 + u\psi^4 + v\psi^6, \tag{5}$$

with $\eta > 0$, $r = \eta c_{os}$, $u > 0$, $v > 0$, and $f_0''(c) > 0$ in some range of concentrations larger than $c_{os}$. An example used later in numerical calculations is

$$f(c,\psi) - \mu c = \psi^2 (1-\psi^2)^2 + 4(\psi^2 - c)^2, \tag{6}$$

with $c_\alpha = 0$, $c_\beta = 1$, and $\psi_\beta = 1$. The contour plot in Fig. 1 is actually based on this expression. Also shown in Fig. 1 is the concentration $c_{cs}$ corresponding to the ''conditional spinodal'' [4] defined by $d^2 f_\beta / dc^2 = 0$. Since in this work we are not interested in the formation of antiphase domains, we restrict ourselves in the following to states $\psi \geqslant 0$.

After this discussion of the essential structure of the free-energy density $f(c,\psi)$, we turn now to the dynamical equations (1) and (2) and rewrite them in dimensionless form. This can be achieved in different ways; in the version prefered here, thermodynamic and kinetic factors remain separated. Lengths will be measured in units of a length $\xi$, i.e., $\mathbf{r}/\xi \to \mathbf{r}$, which for convenience may be chosen as the correlation length of the structural order parameter, $\xi \sim (K_\psi / r)^{1/2}$. Furthermore, we introduce dimensionless order parameters by setting $\psi/\psi_0 \to \psi$, $c/c_0 \to c$, where we require $\psi_0^2 K_\psi = c_0^2 K_c$. The remaining freedom in the order-parameter amplitudes $\psi_0$ and $c_0$ can be used to rescale the analytical expression for the function $f(c,\psi)$. Finally, the replacements $f/(\xi^2 K_c) \to f$ and $t \Gamma_c K_c / \xi^4 \to t$ lead to the following form of Eqs. (1) and (2):

$$\frac{\partial c}{\partial t} = \Delta \left( -\Delta c + \frac{\partial f}{\partial c} \right), \tag{7}$$

$$\frac{\partial \psi}{\partial t} = -\Gamma \left( -\Delta \psi + \frac{\partial f}{\partial \psi} \right), \tag{8}$$

with the dimensionless coefficient

$$\Gamma = \xi^2 \Gamma_\psi K_\psi / \Gamma_c K_c . \tag{9}$$

## III. LINEARIZED THEORY

Within the framework of a linearized theory, we examine the temporal evolution of an initially uniform, stationary state $(\overline{c}, \overline{\psi})$ satisfying $(f_\psi)_{\overline{c},\overline{\psi}} = 0$. Hence the corresponding point $(\overline{c}, \overline{\psi})$ in Fig. 1 either lies on the $c$ axis ($\psi = 0$) or on the curve $\hat{\psi}(c)$. It is convenient to introduce a vector notation

$$\chi(\mathbf{r},t)=\begin{bmatrix} c(\mathbf{r},t) \\ \psi(\mathbf{r},t) \end{bmatrix}, \quad \chi_0=\begin{bmatrix} \overline{c} \\ \overline{\psi} \end{bmatrix}. \tag{10}$$

After linearization with respect to small deviations $\delta\chi$ from the initial state $\chi_0$, Eqs. (7) and (8) are solved by writing

$$\chi(\mathbf{r},t)=\chi_0+\delta\chi\ \exp(i\mathbf{k}\cdot\mathbf{r}+\omega t), \tag{11}$$

which for fixed wave vector $\mathbf{k}$ yields a $(2\times2)$ eigenvalue problem

$$\mathbf{A}\ \delta\chi=-\omega\ \delta\chi, \tag{12}$$

where

$$\mathbf{A}=\mathbf{T}(\mathbf{H}+k^2\mathbf{I}), \tag{13}$$

with

$$\mathbf{T}=\begin{bmatrix} k^2 & 0 \\ 0 & \Gamma \end{bmatrix} \tag{14}$$

and

$$\mathbf{H}=\begin{bmatrix} f_{cc} & f_{c\psi} \\ f_{c\psi} & f_{\psi\psi} \end{bmatrix}. \tag{15}$$

$\mathbf{I}$ is the $(2\times2)$ unit matrix, and the derivatives in Eq. (15) are taken at $\chi_0$. Since $\mathbf{A}$ is a product of two symmetric matrices, with $\mathbf{T}$ positive definite for $k\neq0$, the eigenvalues $\omega_{1,2}$ of $\mathbf{A}$ are real. Explicitly,

$$\omega_{1,2}(k)=-(A_{11}+A_{22}\pm\sqrt{D})/2, \tag{16}$$

with

$$D=(A_{11}-A_{22})^2+4A_{12}A_{21}. \tag{17}$$

For these two ''dispersion branches'' $\omega_{1,2}(k)$, we use in the following the notation $\omega_\pm(k)$, such that $\omega_+(k)>\omega_-(k)$. It should be noted here that unlike the conventional Cahn-Hilliard theory, the behavior of the two branches as a function of $k$ in general depends on $\Gamma$, i.e., on the ratio of the two kinetic coefficients $\Gamma_c$ and $\Gamma_\psi$; cf. Eq. (9). That $k$ dependence can be discussed most directly by considering the following special cases. In the limit $k\to0$ we have the two solutions

$$\omega_1(k)\simeq-(\det\mathbf{H}/f_{\psi\psi})k^2+O(k^4), \tag{18}$$

$$\omega_2(k)\simeq-(\Gamma f_{\psi\psi}+gk^2)+O(k^4), \tag{19}$$

with

$$g=\Gamma+f_{c\psi}^2/f_{\psi\psi}, \tag{20}$$

whose assignment to $\omega_\pm(k)$ will depend on the signs of det $\mathbf{H}$ and $f_{\psi\psi}$. In the opposite limit of large $k$, the two equations (12) become uncoupled, and we find

$$\omega_-(k)\sim-k^4, \tag{21}$$

$$\omega_+(k)\sim-\Gamma k^2. \tag{22}$$

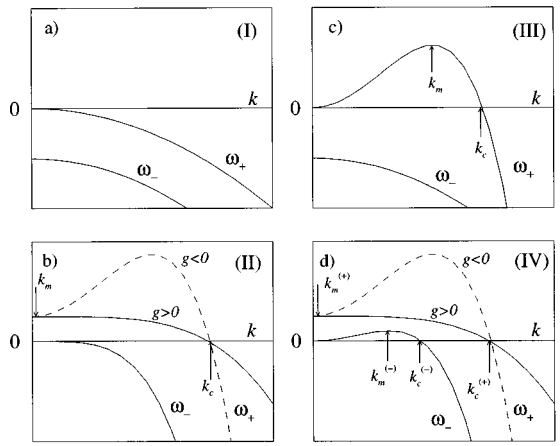


FIG. 2. Schematic behavior of mode spectra for the four possible combinations of sgn($f_{\psi\psi}$) and sgn(det$\mathbf{H}$).

Next we obtain the critical wave numbers $k_c>0$, defined by $\omega_\pm(k_c)=0$. Let $\lambda_1$ and $\lambda_2$ be the eigenvalues of the matrix $\mathbf{H}$. From Eq. (12) it follows immediately that the critical wave numbers are determined by the negative eigenvalues of $\mathbf{H}$: If $\lambda_\nu<0$, then

$$k_{c,\nu}^2=-\lambda_\nu. \tag{23}$$

Therefore the range of unstable fluctuations $0<k<k_{c,\nu}$ in the corresponding branch depends on the coupling $f_{c\psi}$ between order-parameter and concentration modes, but is of course independent of $\Gamma$. We also conclude that the number of unstable branches is given by the number of negative eigenvalues of $\mathbf{H}$.

The above considerations already allow us to classify the possible types of dispersion relations $\omega_\pm(k)$ according to the signs of det $\mathbf{H}=\lambda_1\lambda_2$ and of $f_{\psi\psi}$. Four cases, schematically depicted in Fig. 2, can be distinguished.

### A. case (I): $f_{\psi\psi}>0$, detH>0

These two conditions imply that both eigenvalues $\lambda_{1,2}$ are positive. This is a stable situation, as illustrated in Fig. 2(a).

### B. case (II): $f_{\psi\psi}<0$, detH<0

In contrast to the previous case, $\mathbf{H}$ has one negative eigenvalue. This leads to one unstable branch, whose dispersion relation $\omega_+(k)$ for small $k$ is given by Eq. (19): see Fig. 2(b). Its eigenvector in the limit $k\to0$ only retains a $\psi$ component and thus corresponds to growth of structural order. In the absence of any coupling ($f_{c\psi}=0$), this branch would describe a ''model-A''-like instability [10]; the associated critical wave vector $k_c$ determines a typical length scale $2\pi k_c^{-1}$ of ordered domains in the initial stages of ordering. [If $f_{c\psi}\neq0$, the coefficient $g$, Eq. (20), may turn negative. The unstable branch then behaves as indicated by the dashed line in Fig. 2(b).]

### C. case (III): $f_{\psi\psi}>0$, detH<0

Again, we have one unstable branch [Fig. 2(c)], which now corresponds to Eq. (18), showing that it starts out from zero with positive curvature. Note that in view of $f_\psi=0$ the

coefficient in front of the $k^2$ term in Eq. (18) is equal to $d^2 f_\beta / dc^2$. The eigenvector of the unstable branch is of mixed character for all $k$, which means that in general we encounter simultaneous growth of order-parameter and concentration fluctuations. At $k=0$ the components $\delta c$ and $\delta\psi$ of the eigenvector $\delta\chi$ satisfy $\delta c/\delta\psi = -f_{\psi\psi}/f_{c\psi}$; hence, the eigenvector is tangential to the curve $\hat{\psi}(c)$.

### D. case (IV): $f_{\psi\psi}<0$, detH>0

Here we have two unstable branches, as shown in Fig. 2(d). Again, the case $g<0$ is indicated by the dashed line.

Let us now discuss the physical content of the foregoing analysis by using the free-energy model described in Sec. II. Application of our calculations to a quench from the $\alpha$ phase suggests that different ordering scenarios are possible. Consider first the situation where the evolution starts from a reference state with $\overline{c} > c_{os}$, $\overline{\psi}=0$, and $f_{cc}>0$. Then the primary instability corresponds to case (II), where in our model $g>0$. This is a conventional model-A-type instability, where ordering evolves in a uniform manner with maximum growth at $k_m=0$. Initial fluctuations in the concentration, however, will decay. Of course, the linear approximation breaks down once the condition

$$|\delta\psi_{\mathbf{k}=\mathbf{0}}(t)| = |\delta\psi_{\mathbf{k}=\mathbf{0}}(0)\exp([\omega_+(0)t])| \ll |\psi_\beta| \qquad (24)$$

ceases to be valid. Qualitatively, however, one expects the system to evolve further (beyond the linear regime) along a trajectory in the $(c,\psi)$ plane essentially oriented in the $\psi$ direction, until it reaches some homogeneous stationary state $(c_1,\psi_1)$ with $c_1 \simeq \overline{c}$, $\psi_1 \simeq \hat{\psi}(\overline{c})$, which satisfies $f_{\psi\psi}(c_1,\psi_1) > 0$. Clearly, this kind of description will be applicable only if ''spreading'' of the trajectory remains negligibly small, which requires thermal noise to be negligible and the process to be sufficiently rapid in comparison to phase separation, i.e., $\Gamma \gg 1$. This type of ordering under constant composition (''congruent ordering'') has been analyzed recently by Chen and Khachaturyan in numerical studies of certain discrete alloy models with specific sets of interaction constants [5,6].

Suppose now that the stationary state $(c_1,\psi_1)$ (see above) is taken as the reference state in the foregoing analysis. This state will be metastable if det$\mathbf{H}>0$ [case (I)], such that subsequent equilibration proceeds via nucleation, but it will be unstable if det$\mathbf{H}<0$. The limiting case det$\mathbf{H}=0$ corresponds to the ''conditional spinodal'' [4]. If det$\mathbf{H}<0$, the situation agrees with case (III), which is reminiscent to conventional spinodal decomposition driven by the conditional free energy $f_\beta(c)$. In comparison with the standard Cahn-Hilliard theory, however, some important differences should be noted. Spatial fluctuations in structural order and composition remain coupled, according to the direction of the associated eigenvector. This direction changes with $k$. [In general, it is not tangential to the curve $\hat{\psi}(c)$, apart from $k=0$.] Furthermore, as mentioned before, the spectrum of unstable modes explicitly depends on the parameter $\Gamma$, i.e., on the ratio of kinetic coefficients. To give an example, we plot in Fig. 3 the $\Gamma$-dependent spectra of unstable modes and the associated location of the maximum growth rate $k_m$ in $\mathbf{k}$ space using the free-energy model, Eq. (6), and a reference state $\chi_1$ with components $c_1=0.5$, $\psi_1=\hat{\psi}(c_1)\simeq 0.73$. Note

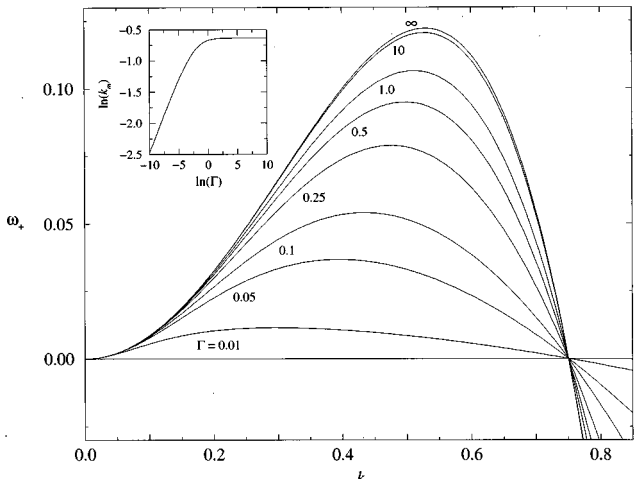


FIG. 3. $\Gamma$ dependence of unstable dispersion branch $\omega_+(k)$ calculated from the model free energy, Eq. (6), and a reference state $c_1=0.5$, $\psi_1=\hat{\psi}(c_1)\simeq 0.73$ [see also Fig. 2(c)]. The inset shows the wave vector $k_m$ corresponding to maximum growth as a function of $\Gamma$.

that $k_m$ as a function of $\Gamma$ appears to display a $\Gamma^{1/4}$ dependence for $\Gamma \ll 1$, whereas $k_m$ becomes constant for $\Gamma \gg 1$.

Our discussion so far in this section suggests that a quench to a state $\overline{c} > c_{os}$, $\overline{\psi}=0$ with $f_{cc}>0$ actually can lead to a sequence of two transformations, if $\Gamma \gg 1$, namely, the buildup of an ordered structure under constant composition and subsequent phase separation into coexisting ordered and disordered domains, accompanied by a relaxation of the order parameters to their respective equilibrium values. Sequences of instabilities are known from experiment [8,9] and from the above-mentioned studies of specific lattice models [5–7]. In order to confirm the appearance of such phenomena within the frame of model C, we have solved numerically the nonlinear equations (7) and (8). Before we turn to that, let us complete our discussion of Fig. 2 and consider the case (IV). A sufficient condition for its occurrence is $f_{\psi\psi}<0$ together with $f_{cc}<0$. Then the two eigenvectors of the matrix $\mathbf{A}$, Eq. (13), in an initial state with $\overline{\psi}=0$ will have the form $(\delta c,0)$ and $(0,\delta\psi)$. We remark that this situation has some bearing on the work by Binder *et al.* [14], who studied spinodal decomposition in the presence of a slowly relaxing (nonconserved) variable $\psi$, which, however, had no dispersion ($K_{\psi=0}$) and hence led to a different form of the mode spectrum at larger $k$.

Experimentally, the dynamics of the transition are often studied with the aid of scattering techniques, which yield information on the time-dependent structure factors,

$$S_{cc}(\mathbf{k},t) = \langle |\delta c_{\mathbf{k}}(t)|^2 \rangle, \quad S_{\psi\psi}(\mathbf{k},t) = \langle |\delta\psi_{\mathbf{k}}(t)|^2 \rangle, \quad (25)$$

defined in terms of the Fourier components $\delta c_{\mathbf{k}}(t)$ and $\delta\psi_{\mathbf{k}}(t)$ of concentration and order-parameter fluctuations. Here averages are taken over the initial fluctuations. Assuming an instantaneous temperature quench, the initial values at $t=0$ in Eq. (25) correspond to the equilibrium structure factors at the temperature $T_i$ before the quench. In addition, we define

$$S_{c\psi}(\mathbf{k},t) = \mathrm{Re}\langle \delta c_{\mathbf{k}}(t)\,\delta\psi_{-\mathbf{k}}(t)\rangle = S_{\psi c}(\mathbf{k},t). \qquad (26)$$

Equations (25) and (26) are readily evaluated either by taking Laplace transforms of the equations of motion, which in a matrix form are [15]

$$\frac{\partial}{\partial t}\mathbf{S}(t) = -[\mathbf{A}\mathbf{S}(t) + \mathbf{S}(t)\mathbf{A}^T], \tag{27}$$

where $\mathbf{A}^T$ denotes the transpose of $\mathbf{A}$, or by directly calculating $\delta c_{\mathbf{k}}(t)$ and $\delta\psi_{\mathbf{k}}(t)$ from the linearized equations of motion. In Eq. (27) and in the rest of this section, we have dropped the variable $\mathbf{k}$ in our notation. The result is

$$S_{cc}(t) = a_+ e^{2\omega_+ t} + b e^{(\omega_+ + \omega_-)t} + a_- e^{2\omega_- t}, \tag{28}$$

with

$$a_\pm = [(A_{11} - \omega_\mp)^2 S_{cc}(0) + 2(A_{11} - \omega_\mp)A_{12} S_{c\psi}(0) + A_{12}^2 S_{\psi\psi}(0)]/D \tag{29}$$

and

$$b = -2[(A_{11} - \omega_+)(A_{11} - \omega_-)S_{cc}(0) + A_{12}(A_{11} - A_{22})S_{c\psi}(0) + A_{12}^2 S_{\psi\psi}(0)]/D. \tag{30}$$

Here $S_{c\psi}(0) = 0$ if the quench is from the $\alpha$ phase.

An analogous expression is found for $S_{\psi\psi}(t)$, which differs from the above expressions by exchanging indices $1 \leftrightarrow 2$ and, correspondingly, $c \leftrightarrow \psi$. As seen from these results, the structure factors display a nonexponential time dependence due to the superposition of three terms involving different rate constants. Their growth or decay with time depends on the behaviors of $\omega_\pm$ summarized in Fig. 2. Apart from case (I) (see above), the first term in Eq. (28) is the most rapidly growing term. The behavior of the second term will be governed by $(\omega_+ + \omega_-) = -[\Gamma f_{\psi\psi} + k^2(\Gamma + f_{cc}) + k^4]$, which can take either sign, whereas the last term will always decay with the exception of case (IV).

## IV. NUMERICAL SIMULATIONS

In this section we present some numerical solutions of the nonlinear equations (7) and (8), using a free energy $f(c,\psi)$ as given by Eq. (6). One purpose of these calculations is to demonstrate that after a quench of the $\alpha$ phase below the ordering spinodal our system can display a sequence of instabilities of the type discussed before, provided that $\Gamma \gg 1$. Such a scenario should be expected from the discussion in the previous section. A quite different behavior, however, will arise for $\Gamma < 1$, which corresponds to slow structural relaxation. Intuitively, since in the $(c,\psi)$ plane the evolution in the $\psi$ direction then is slow and proceeds in a region of the free-energy surface with $\det\mathbf{H} < 0$ (see Fig. 1), we now expect the trajectories to spread initially as a consequence of the fluctuations in the initial state. From the beginning the process will then be characterized by a simultaneous occurrence of ordering and phase separation and will be much more sensitive to fluctuations than in the case $\Gamma \gg 1$.

For a first demonstration of these qualitative issues in the frame of our model, it suffices to study the problem in one dimension. Specifically, we take a system of length $L = 500$ (in units of the correlation length $\xi$), with periodic boundary conditions [16]. Our initial conditions correspond to a mean concentration $\bar{c}$ and random fluctuations $\Delta c = \Delta\psi = 0.05$. Since in this study we are not interested in the formation of antiphase domains, we also include in the initial conditions a small positive bias $\bar{\psi} = 0.05$, which suppresses relaxation towards states with $\psi < 0$. All results for the structure factors are averaged over 300 independent initial configurations.

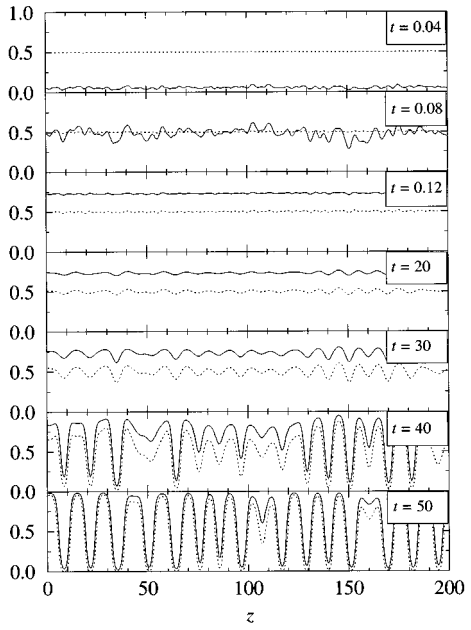


FIG. 4. Simulated patterns $c(z,t)$ (dashed lines) and $\psi(z,t)$ (solid lines) at a series of times for an initial concentration $\bar{c} = 0.5$, $\bar{\psi} = 0$, and $\Gamma = 10$, showing the emergence and the transient persistence of a homogeneously ordered state up to about $t = 10$ and subsequent decomposition.

First, let us consider the case of fast structural relaxation, e.g., $\Gamma = 10$. Figure 4 shows the time evolution of patterns within a section of length 200 of the system. Dashed lines and solid lines represent the concentration $c(z,t)$ and the structural order parameter $\psi(z,t)$, respectively. The initial concentration $\bar{c} = 0.5$ satisfies $c_{os} < \bar{c} < c_{cs}$. Two stages are clearly distinguished. In the first three configurations with $t \lesssim 0.12$, we observe that $c(z,t)$ stays close to the constant $\bar{c}$, whereas $\psi(z,t)$ shows unstable growth and relaxes more or less homogeneously (with larger fluctuations around $t = 0.08$) to a value $\psi_1 \simeq 0.73$. Pictorially, this corresponds in Fig. 1 to a transition in the vertical direction to a state $(c_1, \psi_1)$ with $c_1 \simeq \bar{c}$ on the curve $\hat{\psi}(c)$. This state reached by the process of ''congruent ordering'' [6] persists without notable changes up to a time $t \simeq 10$. For larger times, see the subsequent configurations in Fig. 4, we observe a second instability, initially characterized by coupled small-amplitude concentration and order-parameter fluctuations with a typical wave vector $k_m \simeq 0.52$ (see below). As time proceeds, these fluctuations grow until the system breaks up into a nearly periodic structure of disordered and ordered domains which correspond to the two equilibrium phases $\alpha$ and $\beta$. Comparing the patterns for $t = 40$ and $t = 50$, we also see the onset of coarsening via period doubling [17], which

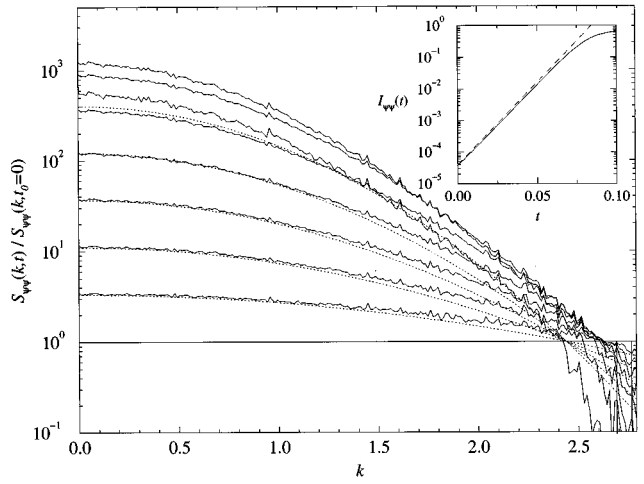


FIG. 5. Normalized time-dependent structure factor $S_{\psi\psi}(k,t)$ for different times $t=0.01$ up to $t=0.08$ in steps of 0.01, using $\overline{c}=0.5$, $\overline{\psi}=0$, and $\Gamma=10$ (see the patterns of Fig. 4). Dotted lines: predictions of the linearized theory. The inset shows the total intensity $I_{\psi\psi}(t)$. The dashed straight line has a slope $2\omega_+(0)$.

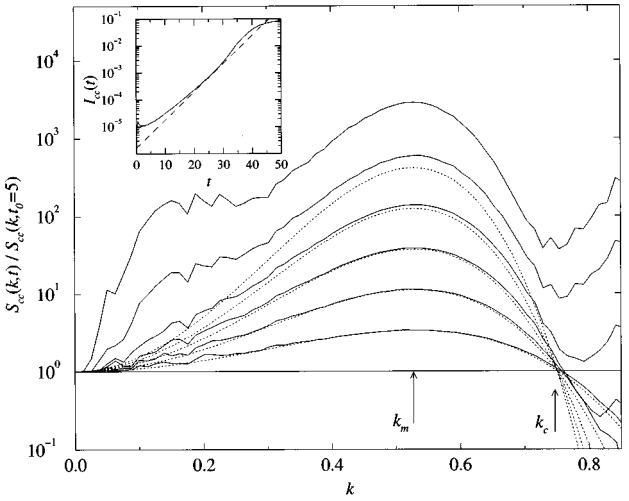


FIG. 6. Normalized time-dependent structure factor $S_{cc}(k,t)$ for different times $t=10$ up to $t=35$ in steps of 5 using the same parameters as in Figs. 4 and 5. [Curves for the larger times display increased statistical fluctuations in $k$ regions where the normalisation factor $S_{cc}(k,t=5)$ is small.] Dotted lines: predictions of the linearized theory with the same reference state as in Fig. 3. Arrows indicate the associated wave vectors $k_m\simeq 0.52$ and $k_c\simeq 0.75$. The inset shows the total intensity $I_{cc}(t)$. The dashed straight line has a slope $2\omega_+(k_m)$.

is an effect specific to one dimension.

In their respective short-time regimes, the two instabilities displayed in Fig. 4 can be related to the predictions of the linearized theory with reference states $\chi_0=(\overline{c},0)$ and $\chi_1=(\overline{c},\psi_1)$, respectively. To show this we first plot in Fig. 5 the structure factor $S_{\psi\psi}(k,t)$ normalized with respect to $S_{\psi\psi}(k,0)$ on a logarithmic scale, for a series of times up to $t=0.08$. These results are compared with the linearized theory of Sec. III (see the dotted lines), which simply gives $\ln[S_{\psi\psi}(k,t)/S_{\psi\psi}(k,0)]\simeq 2\omega_+(k)t$ as the leading contribution. Here $\omega_+(k)$ is calculated with respect to the reference state $\chi_0$. This yields $k_c\simeq 2.4$ and a maximum growth rate at $k_m=0$ [see the behavior of the unstable branch in Fig. 2(b)]. Good quantitative agreement is found in Fig. 5 up to times $t\sim 5\times 10^{-2}$. The inset shows a corresponding comparison between the simulated total intensity,

$$I_{\psi\psi}(t)=\sum_k S_{\psi\psi}(k,t). \tag{31}$$

and the approximate result $\ln I_{\psi\psi}(t)\sim 2\omega_+(0)t$ of the linearized theory.

An analogous comparison can be made for the second instability. As ''initial'' time we choose $t_0=5$, where the system is close to a homogeneously ordered state characterized by $\chi_1$ (cf. Fig. 4). In order to eliminate the unknown fluctuations in that state, we study the evolution of $S_{cc}(k,t)$ normalized with respect to $S_{cc}(k,t_0)$. Apart from small $k$, Fig. 6 essentially confirms a growth according to the predictions of the linearized theory, $\ln[S_{cc}(k,t)/S_{cc}(k,t_0)]\simeq 2\omega_+(k)(t-t_0)$, as long as $t\lesssim 30$. The growth rate $\omega_+(k)$ is calculated here from the reference state $\chi_1$ and corresponds to the upper dispersion branch in Fig. 2(c). In particular, the location of the wave vector $k_m\simeq 0.52$ for maximum growth and the critical wave vector $k_c\simeq 0.75$ nicely agrees with the linearized theory (see the arrows in Fig. 6). This comparison, of course, becomes meaningless for longer times $t\gtrsim 30$, where the structure factor appears to develop a second peak near $k_m/2$, which reflects period doubling. We also calculated the integrated intensity $I_{cc}(t)=\Sigma_k S_{cc}(k,t)$, which is compared in the inset with the leading behavior according to the linearized theory $\ln I_{cc}(t)\sim 2\omega_+(k_m)(t-t_0)$.

Next, we turn to the situation of slow structural relaxation and choose $\Gamma=0.1$, $\overline{c}=0.5$. Our calculations show that spatial fluctuations in $c(z,t)$ and $\psi(z,t)$ now evolve simultaneously. These fluctuations have a considerably larger amplitude than in Fig. 4 for times $t\lesssim 30$, and the patterns appear more irregular. This can be understood qualitatively from the aforementioned ''spreading'' of trajectories, which is illustrated in Fig. 7. Starting from one particular configuration of

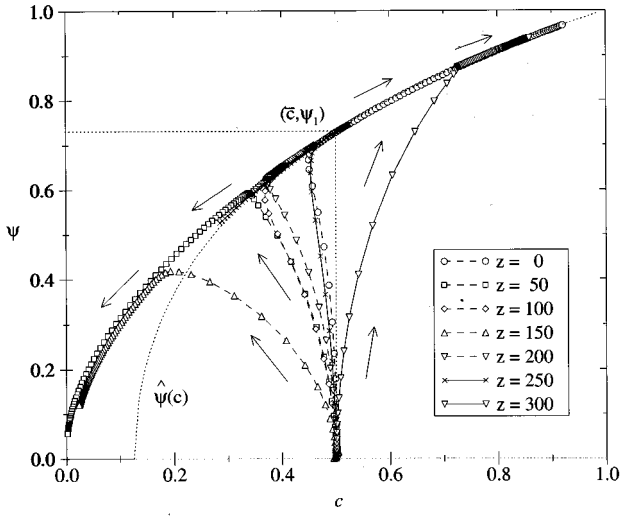


FIG. 7. Spread of trajectories in the $(c,\psi)$ plane due to fluctuations, for $\Gamma=0.1$ (see text).

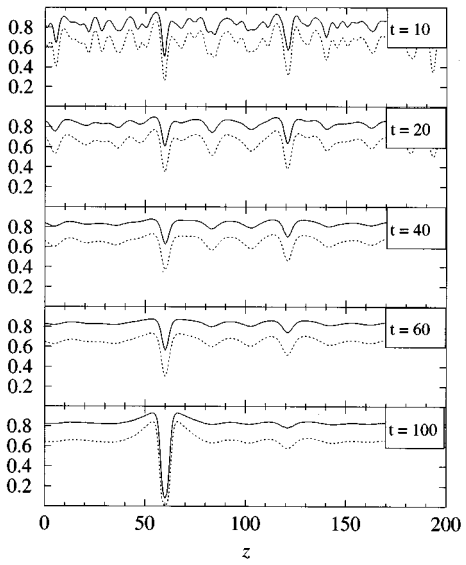


FIG. 8. Simulated patterns $c(z,t)$ (dashed lines) and $\psi(z,t)$ (solid lines) at different times for $\overline{c}=0.65>c_{cs}=0.625$ and $\Gamma=0.1$.

initial fluctuations, we plotted pairs of calculated values $c(z,t)$, $\psi(z,t)$ for some fixed $z$, while time progresses in steps $\Delta t=0.5$, which yields a discrete trajectory. Repeating this construction for different $z$ leads to a set of trajectories which evolve under increasing their mutual distances, before they reach a common curve. This curve can be shown to be closely related to the equilibrium profile of a free interface between the $\alpha$ and $\beta$ phases, which satisfies $\delta F/\delta c=0$, $\delta F/\delta\psi=0$. [By contrast, if the same analysis were done for $\Gamma=10$ and for the same initial fluctuation amplitudes, then all such trajectories almost would collapse until they reach the curve $\hat{\psi}(c)$ at a rather well-defined point $\overline{c}\simeq 0.5$, $\psi_1\simeq 0.73$.] The whole process for $\Gamma=0.1$ can be regarded as spinodal decomposition where the initial fluctuations are amplified strongly through the concurrent nonlinear structural relaxation. As a consequence, one can show that the structure factor $S_{cc}(k,t)$ displays a much broader distribution than in Fig. 6 and that the linearized theory fails to describe $S_{cc}(k,t)$ in any time interval.

A particularly interesting situation occurs when the initial concentration is outside the conditional spinodal region, $\overline{c}>c_{cs}$. For large $\Gamma$ the initial ordering process will then lead to a homogeneous metastable state. However, for small $\Gamma$, part of the trajectories will reach the unstable region of the curve $\hat{\psi}(c)$ and initiate phase separation. This is seen from the patterns in Fig. 8, which were calculated for $\overline{c}=0.65$ and $\Gamma=0.1$. There a localized fluctuation is observed which for increasing time becomes a nucleus of the disordered phase, while the rest of the system relaxes towards $c$ and $\psi$ values which correspond to the metastable part of the curve $\hat{\psi}(c)$. For a given magnitude of the initial fluctuations, the frequency of the occurrence of such $\alpha$-phase nuclei and the associated length scale depends sensitively on $\Gamma$. It follows that the quantity $c_{cs}$ loses its physical significance as that concentration which separates the metastable from the unstable part of the curve $\hat{\psi}(c)$, when $\Gamma$ becomes small. The fact that fluctuations generally prevent a precise location of a spinodal was emphasized long ago by Binder [18]. As indicated above, the relevant fluctuations here are not just the equilibrium fluctuations in the state before the quench, but amplified fluctuations, which grow as $\Gamma$ becomes smaller.

Finally, we also calculated the structure factor $S_{cc}(k,t)$ related to the patterns in Fig. 8. For $t\lesssim 20$ it develops a main peak at a wave vector which reflects the typical spatial extension of $\alpha$-phase nuclei. Additional calculations for much larger times (up to $t\simeq 10^3$) show that these nuclei undergo diffusive growth and that the main peak in $S_{cc}(k,t)$ shifts to smaller wave vectors. At the same time $\beta$-phase domains develop from the rim of $\alpha$-phase nuclei. Phase separation, initiated at very short times by a spinodal mechanism, thus proceeds via growth of $\alpha$ and $\beta$ domains out of a metastable background. In principle, such considerations might apply to quench experiments in alloys, where the state right after the quench is close to the conditional spinodal.

## V. SUMMARY AND CONCLUSIONS

We investigated some general aspects in the early-time kinetics of ordering and phase separation within coupled time-dependent Ginzburg-Landau equations of the type of model C [10]. This model provides a simple, yet general frame for discussing different ordering scenarios as detected previously in kinetic mean-field theories for specific alloy models [4–7] and in addition allows us to demonstrate the importance of kinetic effects in determining the time-dependent structure factors.

In particular, after introducing properly scaled variables, we first showed that the linearized theory naturally leads to a classification of different types of instabilities in terms of properties of the free-energy density surface. Some features in the kinetics of decomposition in qualitative distinction to conventional Cahn-Hilliard theory were pointed out, such as an influence of the kinetic coefficients on the dispersion relation of linear modes through the parameter $\Gamma$ and a nonexponential time dependence of the structure factors. Numerical calculations for a simplified nonlinear model revealed a sequence of two instabilities, which in the case of fast structural relaxation (large $\Gamma$) occur on separated time scales. Both of these instabilities are well described by an associated class of dispersion branches of the linearized theory. On the other hand, if $\Gamma$ is small, the observed patterns can be interpreted via spinodal decomposition subject to enhanced fluctuations. This enhancement has its origin in the preceeding nonlinear evolution of structural order. As a consequence, the distinction between ''secondary'' spinodal decomposition and nucleation gets obscured as the initial concentration before the quench, $\overline{c}$, is close to the concentration $c_{cs}$.

We expect that these qualitative conclusions concerning the early-time kinetics should also hold for systems in two or three dimensions, although our basic model may not directly be applicable to real experiments. One limitation of the model C equations (1) and (2) lies in the fact that they provide only the simplest type of coupling between two order parameters. In fact, it has been shown that kinetic mean-field theories applied to lattice models of phase ordering normally lead to more general couplings [19,7]. For example, the equation of motion for $\psi$ can contain additional terms proportional to $\Delta(\delta F/\delta\psi)$ and to $\Delta(\delta F/\delta c)$ [20]. Other impor-

tant effects ignored here may arise from long-range elastic interactions or from a dependence of the kinetic coefficients on the instantaneous nonequilibrium state. Nevertheless, the present work may indicate the possibility to extract information on the kinetic coefficients from the experimentally observed structure, e.g., by analyzing and comparing length scales and time scales, which govern the process of homogeneous ordering and decomposition. More generally, we have found that in a model of coupled conserved and nonconserved order parameters the relative magnitude of the respective kinetic coefficients can have a profound influence on the observed structures at early times.

## ACKNOWLEDGMENTS

The authors have greatly benefited from discussions with Z. Akcasu, H. L. Frisch, P. Maass, A. Majhofer, and J. Reinhard. This work was supported in part by the Deutsche Forschungsgemeinschaft, SFB 513.

## APPENDIX

The mode analysis of Sec. III can be generalized to the case where states $\pm\psi$ are no longer equivalent, $f(c,\psi) \neq f(c,-\psi)$, hence allowing an additional coupling term proportional to $(\nabla c)\cdot(\nabla\psi)$ in the expression (3) for the free-energy functional $F$. Such a coupling may arise from nonlocal interactions between the variable $\psi$ and the concentration $c$. Instead of Eqs. (7) and (8) the rescaled equations of motion now take the form

$$\frac{\partial\psi}{\partial t} = -\Gamma\left(-\Delta\psi - \gamma\Delta c + \frac{\partial f}{\partial\psi}\right), \tag{A1}$$

$$\frac{\partial c}{\partial t} = \Delta\left(-\Delta c - \gamma\Delta\psi + \frac{\partial f}{\partial c}\right), \tag{A2}$$

where the dimensionless parameter $\gamma$ measures the strength of that coupling.

Following Sec. III, the matrix **A** after linearization is now replaced by $\mathbf{T}(\mathbf{H}+k^2\sigma)$, with

$$\sigma = \begin{bmatrix} 1 & \gamma \\ \gamma & 1 \end{bmatrix}. \tag{A3}$$

Thermodynamic stability against fluctuations with finite wave vectors requires $\sigma$ to be positive definite, i.e., $\gamma^2<1$. It is easily seen that expressions (18), (19), and (21) remain unaffected by $\gamma$, whereas Eq. (22) changes into $\omega_-(k) \sim\Gamma(1-\gamma^2)k^2$. Furthermore, in analogy to Eq. (23), the critical wave numbers are now determined by the negative eigenvalues of $\mathbf{H}\sigma^{-1}$. Since $\gamma^2<1$, there is a one-to-one correspondence between negative eigenvalues of **H** and those of $\mathbf{H}\sigma^{-1}$. Hence, although $\omega_\pm(k)$ and the critical wave numbers do depend on $\gamma$, the number of unstable branches is independent of $\gamma$ and follows the same criteria as in Sec. II. This shows that the classification of mode spectra according to the possible combinations of $\mathrm{sgn}(f_{\psi\psi})$ and $\mathrm{sgn}(\det\mathbf{H})$ [see Figs. 2(a)–2(d)] also holds for $\gamma\neq 0$.

[1] For recent reviews, see *Solids Far from Equilibrium*, edited by C. Godreche (Cambridge University Press, Cambridge, England, 1992); *Phase Transformations in Materials, Materials Science and Technology*, Vol. 5, edited by P. Haasen (VCH Weinheim, New York, 1991).
[2] K. Binder, W. Kinzel, and D. P. Landau, Surf. Sci. **117**, 232 (1982).
[3] J. K. G. Dont, *An Introduction to Dynamics of Colloids* (Elsevier, Amsterdam, 1996).
[4] S. M. Allen and J. W. Cahn, Acta Metall. **24**, 425 (1976).
[5] A. G. Khachaturyan, T. F. Lindsey, and J. W. Morris, Jr., Metall. Trans. A **19**, 249 (1988).
[6] Long-Quing Chen and A. G. Khachaturyan, Phys. Rev. B **46**, 5899 (1992).
[7] V. Yu. Dobretsov, V. G. Vaks, and G. Martin, Phys. Rev. B **54**, 3227 (1996).
[8] J. Lendvai and H. J. Gudladt, Z. Metallkd. **84**, 242 (1993).
[9] B. Noble and A. J. Trowsdale, Philos. Mag. A **71**, 1345 (1995).
[10] P. C. Hohenberg and B. I. Halperin, Rev. Mod. Phys. **49**, 435 (1977).
[11] K. R. Elder, B. Morin, M. Grant, and R. C. Desai, Phys. Rev. B **44**, 6673 (1991).
[12] A. M. Somoza and C. Sagui, Phys. Rev. E **53**, 5101 (1996).
[13] C. Sagui, A. M. Somoza, and R. C. Desai, Phys. Rev. E **50**, 4865 (1994).
[14] K. Binder, H. L. Frisch, and J. Jäckle, J. Chem. Phys. **85**, 1505 (1986).
[15] J. Jäckle and M. Pieroth, J. Phys. Condens. Matter **2**, 4963 (1990).
[16] The grid spacing $\Delta z$ is chosen as $\Delta z=\xi/2$, which is much smaller than $2\pi/k_c$ in the cases studied here. For the integration in time, we used a Runge-Kutta algorithm with adaptive stepsize control.
[17] J. S. Langer, Ann. Phys. (N.Y.) **65**, 53 (1971).
[18] K. Binder, Phys. Rev. A **29**, 341 (1984).
[19] G. Martin, Phys. Rev. B **50**, 12 362 (1994).
[20] In the present continuum theory, kinetic couplings of the type discussed in Refs. [19] and [7] would lead to additional terms $\sim O(k^2)$ in the matrix **T**, Eq. (14). This would modify the mode spectra shown in Fig. 2 to order $k^2$. Since **T** remains positive definite, our conclusions with respect to the number of unstable branches and with respect to the critical wave numbers $k_c$ would, however, remain unchanged.